

INTERACTION OF POLARIZED LIGHT WITH CHALCOGENIDE GLASSES

V. Lyubin, M. Klebanov

Physical Department, Ben-Gurion University, Beer-Sheva 84105, Israel

In the first part of the paper we summarize the results of our study of photoinduced optical anisotropy in thin film and bulk samples of different chalcogenide glasses. We distinguish three ranges of exciting photons energy: above-band-gap excitation, sub-band-gap excitation and super-band-gap excitation. We claim that in each of these excitation ranges, different mechanisms are responsible for appearance of photoinduced anisotropy, namely, creation and next orientation of photoinduced defects, creation of anisotropically scattering defects and orientation of main covalent bonds of the glass (in addition to creation and orientation of defects) are the main reasons of observed anisotropy in the mentioned spectral ranges. We consider also some interesting results obtained recently in different research groups. Among them: polarization-dependent photocrystallization of some amorphous films, polarization-dependent photodoping of chalcogenide films by metals, photoinduced anisotropy of photoconductivity, polarization-dependent optomechanical effect and photoinduced anisotropy in the ion-conducting amorphous chalcogenide films.

(Received May 31, 2001; accepted June 11, 2001)

Keywords: Photoinduced optical anisotropy, Chalcogenide glass

1. Introduction

Investigation of interaction of polarized light with chalcogenide glasses continues already more than twenty years, after discovery of the linearly polarized light induced anisotropy in several chalcogenide glassy films made by Zhdanov, Kolomiets, Lyubin and Malinovskii [1,2]. Many research groups studied photoinduced anisotropy (linear dichroism, linear birefringence) and also photoinduced gyrotropy (circular dichroism, circular birefringence, optical activity) excited by linearly polarized light or circularly polarized light in thin films and in bulk chalcogenide glasses. Main results of these studies can be found in [3-10]. Later, some new effects were discovered at studying of interaction of polarized light with chalcogenide glasses: polarization-dependent photodoping of chalcogenide films by silver [12], polarization-dependent photocrystallization of some amorphous chalcogenide films [13-15], polarization-dependent optomechanical effect [16] etc.

In first publications, the photoinduced anisotropy (PA) in chalcogenide films was explained by interaction of polarized light with some optically anisotropic structural elements whose optical axes are oriented randomly [1,2]. Later, more detailed models of PA in thin chalcogenide films were proposed that are based on consideration of interaction of the inducing light with native quasiaatomic defects [17], with quasimolecular defects [18], with bistable centers having a wide distribution of relaxation times [19] or with valence-alteration pairs (VAP's) [20]. An electronic model, in which PA is attributed to photogeneration and trapping of oriented geminate electron-hole pairs in chalcogenide glass, was also proposed recently [21].

In this paper we try to summarize and discuss the recent results of PA study performed mainly in the laboratory of amorphous semiconductors in the Ben-Gurion University (Beer-Sheva, Israel) either independently or in close cooperation with colleagues from other research centers. It is convenient for us to consider and discuss successively the data on PA obtained at excitation by above-band-gap light, sub-band-gap light and super-band-gap light. Additionally we will consider the other effects of polarized light studied recently, including the case of observation of photoinduced photoelectrical anisotropy.

2. Experimental

Two groups of samples were investigated in this research. Thin-film glassy samples of As_2Se_3 , $\text{As}_{50}\text{Se}_{50}$, As_2S_3 , $\text{GeS}_{2.2}$, Se , $\text{Se}_{80}\text{Te}_{20}$ and $\text{Ge}_x\text{As}_{40-x}\text{S}_{60}$ were produced by thermal evaporation of starting glassy materials from usual quartz crucibles onto suitably cleaned Corning glass substrates in vacuum ($p \sim 10^{-6}$ Torr). The $\text{Se}_{70}\text{Ag}_{15}\text{I}_{15}$ films were prepared by evaporation from a vaporiser with a small opening [22]. The film thickness was 0.3-4.0 mm. Bulk samples of As_2S_3 , As_2Se_3 , $\text{Ge}_{20}\text{As}_{20}\text{S}_{60}$ and $\text{As}_{34}\text{S}_{52}\text{I}_{14}$ were prepared by polishing of melt-quenched chalcogenide glasses and had typical thickness of several millimeters.

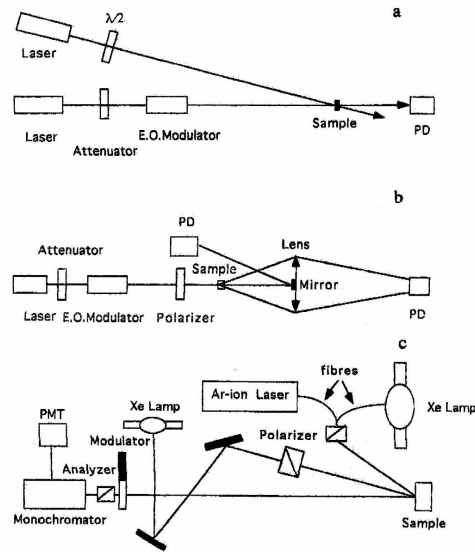


Fig. 1. Experimental installations for investigation of photoinduced anisotropy of absorption (a) scattering (b) and reflection (c) of laser light.

Optical setups used in our experiments are shown schematically in Fig.1. The set-up of Fig. 1a was used for investigation of linear dichroism and linear birefringence in the thin film samples at excitation by above-band-gap light. Two beams of gas lasers illuminate simultaneously the same area of the studied film. The wavelength of one laser is selected so that it is the above-band-gap light. It is an inducing laser beam. The linear polarization state of this beam could be changed to the orthogonal one with a half wave plate. The attenuated light beam from the other laser (probing laser beam) passed through an electrooptical modulator, which modulated the polarization discontinuously between two orthogonal states at a frequency of 1kHz. Then this laser beam was passed through the sample and was incident on the Si photodiode, permitting to measure the photoinduced transmission anisotropy $T_y - T_x = 2(I_y - I_x) / (I_y + I_x)$, where I_y and I_x are the intensities of the beams with two orthogonal electric vectors. To measure the difference signal $I_y - I_x$ we used the method of synchronous detection. If the wavelength of second laser is selected so that it is also the above-band-gap light, we can measure the photoinduced dichroism. In order to study the photoinduced birefringence, the wavelength of second laser must be selected in the range of transparency of the studied film. Usually we used the He-Ne lasers, working at $\lambda = 633$ nm and the Ar^+ lasers, working at $\lambda = 515$ nm. This set-up permitted us to study very initial periods of PA kinetics and relaxation. For study of PA of transmission in the bulk chalcogenide samples excited by sub-band-gap light, we also used the installation of Fig. 1a. Additionally for simultaneous measurement of the laser radiation transmitted through the bulk sample and radiation scattered by the sample to various angles up to 230 mrad. We used the set-up shown in Fig. 1b. Collecting lens, arranged behind the sample, focused the scattered light to a photodiode, and a small mirror, fixed in the central part of the lens, reflected the transmitted light beam to a second photodiode. He-Ne laser radiation ($\lambda = 633$ nm) which was sub-band-gap radiation for the studied bulk glass samples (As_2S_3 glass) played in this installation, by turns, a role of inducing or probing

light. This installation allowed us to study both anisotropy and gyrotropy of transmission and scattering of linearly and circularly polarized light in bulk samples.

The experimental set-up for reflectance difference measurements is shown in Fig. 1c. It is again the two-beams installation. The anisotropy in this case was induced using the light of either a 1000 W Xenon lamp which generated radiation in a wide energy range, including sub-band-gap and super-band-gap light, or an Ar⁺ ion laser ($\lambda = 488$ nm) generating above-band-gap light for the studied samples. The inducing light passed through a Glan-prism polarizer and besides the light intensity on the surface of the sample was around 100 mW/cm². The intensity of the measuring linearly polarized light, generated by small Xenon lamp, was much smaller (about 5 mW/cm²). Application of a monochromator allowed to investigate the spectra of PA of light reflection. For a detailed acquaintance with the reflection-difference spectroscopy see Ref.23.

3. Results and discussion

3.1. Above-band-gap light excitation

Most of early experiments on the PA were performed in the regime of above-band-gap light excitation of thin film chalcogenide glassy samples. Both photoinduced linear dichroism and photoinduced linear birefringence generation and multiple reorientation were revealed under action of linearly polarized light. PA could be decreased to zero at the next irradiation by non-polarized or circularly polarized light.

The best from the different models of PA generation at above-band-gap light excitation is, in our opinion, the model of Tikhomirov and Elliott [20], which is based on the photoinduced orientation of VAP's, the charged defects with negative correlation energy, characteristic for chalcogenide glasses. It is known that there are natural VAP's and photoinduced VAP's in chalcogenide glasses. Our experiments show that photoinduced VAP's play especially important role in generation of PA at above-band-gap light excitation [24].

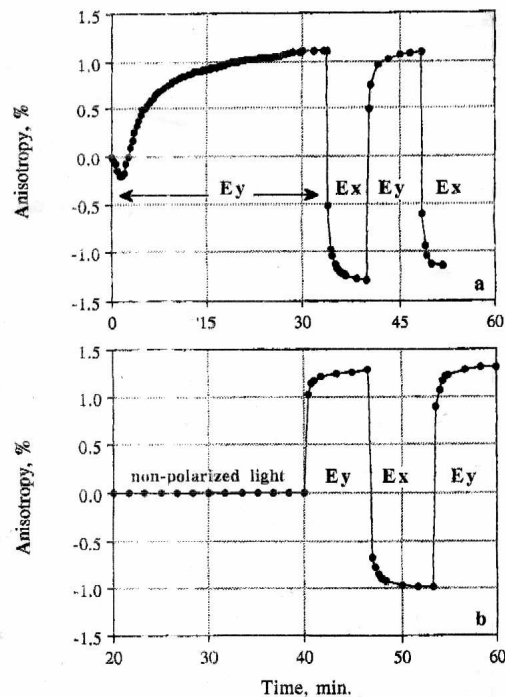


Fig. 2. Kinetics of dichroism generation and reorientation in As₅₀Se₅₀ film under action of linearly polarized laser light with two orthogonal directions of electrical vector (y and x), when reorientation starts after dichroism saturation (a) or when polarized light irradiation starts after long illumination with unpolarized light (b).

The process of photoinduced dichroism generation and reorientation is illustrated in Fig. 2 for the case of the AsSe film of 1.2 μm thickness. It is seen from Fig. 2a that the initial dichroism generation is rather prolonged (10-20 min), while the dichroism reorientation happens much quicker (< 1 min). In the case of long film irradiation with the unpolarized light, the following irradiation with linearly polarized light results in the rapid appearance of dichroism as it is shown in Fig. 2b. Similar peculiarities in the kinetics of dichroism generation and reorientation were observed also in amorphous $\text{As}_{45}\text{Se}_{55}$, As_2S_3 and Ge_2PbS_4 films.

These data and other results described in [24] show that irradiation with both polarized and non-polarized above-band-gap light creates in the non-irradiated film some centers that can be oriented quickly by the subsequent irradiation by linearly polarized light (in case of initial irradiation with the polarized light, these centers are oriented quickly during irradiation). Such centers can be born in the form of VAP's (photoinduced VAP's) in the reaction [25]:



In all previous experiments the authors investigated PA in chalcogenide films that are characterized by the scalar photoinduced effect, photodarkening, when transparency of the sample decreases under light irradiation. At the same time, in some Ge containing chalcogenide glassy films, initial light irradiation induces photobleaching instead of photodarkening. Subsequent light irradiation carried out after annealing of photobleached films results in photodarkening. Photobleaching was investigated in detail in the three-component chalcogenide Ge-As-S films [26,27].

We investigated PA in photobleached $\text{Ge}_{25}\text{As}_{15}\text{S}_{60}$, $\text{Ge}_{32}\text{As}_8\text{S}_{60}$ and $\text{Ge}_{36}\text{As}_4\text{S}_{60}$ films in which large photoinduced changes were observed and studied previously [26]. The results were qualitatively identical for all three studied films and we will illustrate them for the case of $\text{Ge}_{32}\text{As}_8\text{S}_{60}$ films. Fig. 3 shows the typical kinetics of dichroism generation and reorientation in both as-prepared and annealed films. A 2.5 W/cm^2 linearly polarized Ar^+ laser beam at 488 nm with two orthogonal directions of electrical vector was used in these experiments. A 0.5 mW/cm^2 linearly polarized 515 nm Ar^+ laser beam was applied as a probe beam.

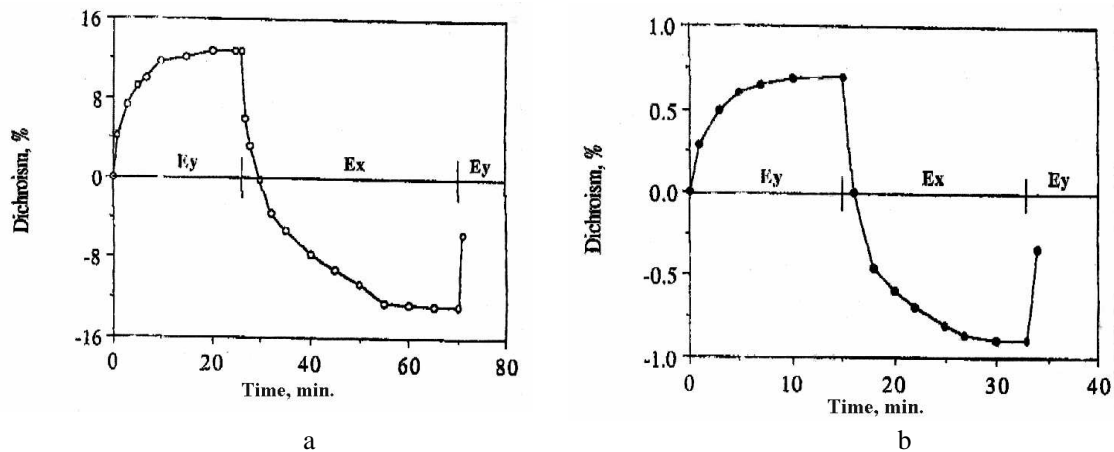


Fig. 3. Kinetics of dichroism generation and reorientation in as-prepared (a) and annealed at 210 $^{\circ}\text{C}$ (b) $\text{Ge}_{32}\text{As}_8\text{S}_{60}$ glassy film, measured by 515 nm probing laser beam.

Quantitative results of photoinduced dichroism study are summarized in Table 1. It is seen that the values of PA in $\text{Ge}_{25}\text{As}_{15}\text{S}_{60}$ and $\text{Ge}_{32}\text{As}_8\text{S}_{60}$ are approximately the same but for $\text{Ge}_{36}\text{As}_4\text{S}_{60}$ films smaller PA values are observed. We can say that the value of the photoinduced dichroism in as-prepared photobleached films (10-15%) is substantially larger than that in most of the previously studied elementary or binary chalcogenide glassy films. Annealing of such films does not result in change of the sign of dichroism. However, the value of dichroism is considerably smaller in annealed films. In this respect, the studied films differ essentially from the binary films where dichroism decreases after annealing very weakly. Generation and reorientation of birefringence was also observed and studied in these photobleached films.

Table 1. The photoinduced dichroism values (in %) for $\text{GeAs}_{(40-x)}\text{S}_{60}$.

	$\text{Ge}_{36}\text{As}_4\text{S}_{60}$	$\text{Ge}_{32}\text{As}_8\text{S}_{60}$	$\text{Ge}_{25}\text{As}_{15}\text{S}_{60}$
As - prepared	3 - 4	12 - 15	8 - 15
Annealed	1 - 2	0.6 - 0.8	-

Summarizing the obtained results, we conclude that characteristics of PA do not depend on photodarkening or photobleaching observed in the as-prepared chalcogenide glassy films. More details about the study of the photobleached films could be found in [28].

3.2. Sub-band-gap light excitation

In early experiments on interaction of linearly polarized and circularly polarized sub-band-gap light with bulk chalcogenide glassy samples about 1 cm thick, several photoinduced phenomena: anisotropy, gyrotropy and light-scattering were discovered and studied [4 and literature cited there]. It was shown also that the polarization state of the light changed essentially as it passed through bulk samples: both rotation of the plane of polarization (optical activity) and ellipticity were seen to occur [4]. Photoinduced linear and circular dichroism and birefringence were shown to be comparable in magnitude and to be responsible for the occurrence of elliptical dichroism and birefringence. These effects were observed and studied later in direct experiments when the bulk samples were irradiated by the elliptically polarized laser light with different ellipticity [29,30].

In the next series of investigations, we measured the linearly polarized or circularly polarized laser radiation transmitted through the bulk sample and radiation scattered by the sample to various angles up to 230 mrad [31,32]. In these experiments we used the set-up shown in Fig. 1b.

We studied the kinetics of change of scattered light intensity induced by strong linearly polarized or circularly polarized radiation with two orthogonal directions of electrical vector (E_y - radiation and E_x - radiation, E_r - radiation and E_l - radiation). It was shown that the E_y -radiation, for example, induces an increase of scattering of the corresponding (I_y) light. Simultaneously, the intensity of I_x light usually decreases. On the contrary, the E_x - radiation induces a decrease of I_y light and a growth of I_x light. The analogous results were recorded in the case of circularly polarized light.

Fig. 4 and 5 show a typical kinetics of photoinduced changes of the scattered and transmitted light anisotropy and also of the scattered and transmitted light gyrotropy. It is seen from the figures that scattering anisotropy (gyrotropy) and transmittance anisotropy (gyrotropy) always change in opposite directions: an increase of one of them is accompanied by the decrease of the other one and vice versa. The anisotropy (gyrotropy) of scattering and transmittance were shown to remain practically invariant during at least 3 - 5 hours.

In some experiments the sample was first excited by non-polarized light and only then was irradiated by linearly or circularly polarized radiation. Non-polarized radiation induced additional isotropic light scattering, while the subsequent linearly or circularly polarized radiation resulted in appearance of scattering anisotropy or gyrotropy which could be reoriented. This peculiarity is demonstrated in Fig. 5 for the case of photoinduced gyrotropy.

Obtained quantitative data about the photo-induced light scattering anisotropy and gyrotropy permit us to draw some interesting conclusions. The oppositely directed changes of photoinduced anisotropy (gyrotropy) of transmittance and scattering allow us to assume that the creation of anisotropically or gyrotropically scattering centers is the basis of the whole group of photoinduced vectorial phenomena in bulk chalcogenide glasses excited by the sub-band-gap light. The energy of corresponding light quanta is not sufficient for breaking the interatomic covalent bond, but sufficient to produce some changes in the system of weaker bonds, for example, intermolecular Van der Waals bonds or the so-called three-center bonds [18]. These changes can result in the appearance of scattering centers in the glass. Such centers will scatter the light isotropically, anisotropically or gyrotropically depending on the polarization state of the inducing radiation. The anisotropy (gyrotropy) of such centers can be reoriented when the polarization state of the inducing radiation is changed.

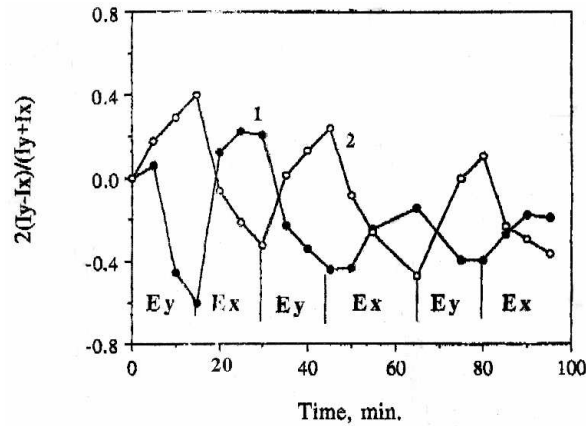


Fig. 4. Kinetics of transmittance anisotropy (1) and scattering anisotropy (2) changes in an As_2S_3 bulk glass sample induced by E_y and E_x laser radiation.

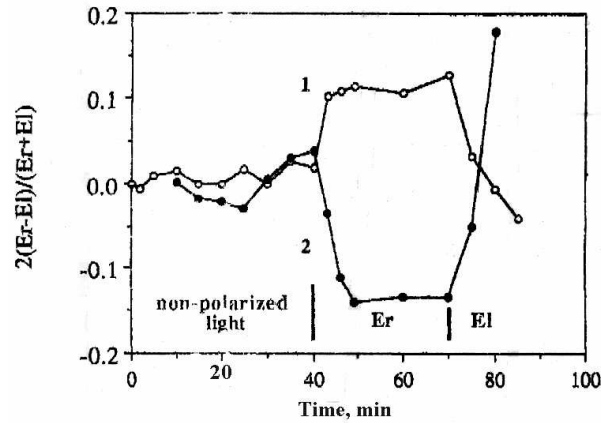


Fig. 5. Kinetics of scattered gyrotropy (1) and transmittance gyrotropy (2) changes in an As_2S_3 bulk glass sample induced by E_r and E_l laser radiation.

3.3. Super-band-gap light excitation

Interaction of super-band-gap photons with chalcogenide glass could not be studied using the transmittance measurements because of strong light absorption. In this case we applied the reflectance-difference spectroscopy which allowed us to investigate the photoinduced anisotropy in glassy samples both thin films and bulks in a broad spectral range [33]. In these experiments we used the set-up shown in Fig. 1c. The measured value is defined as $Dr/r = 2(r_y - r_x)/(r_y + r_x)$, where r_y and r_x are the reflectance values for the polarization of the probing beam in the direction parallel or perpendicular to the polarization of the inducing beam.

Main new results, obtained in this research, were the observation of anisotropy excited by photons with energy substantially exceeding the band-gap of the chalcogenide glass and observation of PA at energies much higher than the energy of exciting photons.

Fig. 6 shows the PA of light reflection in the bulk As_2S_3 induced by the linearly polarized light of Xe lamp or Ar^+ laser. It is seen that the PA is appeared in the whole 1.5-5.0 eV range. Interesting that for the glass excited by Xe-lamp light the trend in the reflectance change was the same (increase or decrease depending on the polarization) throughout the whole studied spectral range. At the same time, in case of the Ar^+ laser excitation, sign variation of the effect is clearly recorded. The increase in Dr/r is observed for larger photon energies (above 4.0 eV) similar to the previous case of polychromatic light excitation, but for smaller photon energies an opposite change (decrease) is detected. It is seen also that a change of the light polarization to the orthogonal one results in a reversal of the PA with the same crossover energy of 4.0 eV. All peculiarities of PA of reflection were shown to be characteristic not only for As_2S_3 glass but also for all chalcogenide glasses studied.

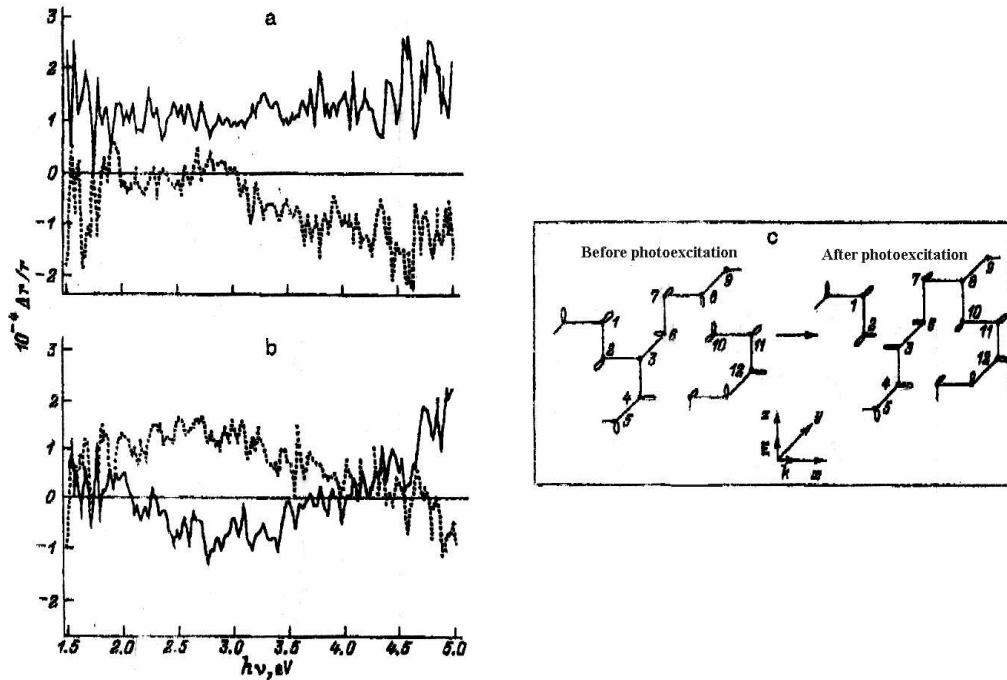


Fig. 6. Photoinduced reflectance anisotropy (solid lines) and its reorientation (dotted lines) in an As_2S_3 bulk glass sample irradiated by the light of 1000 W Xe lamp (a) or Ar^+ ion laser (b) and schematic representation of photostructural changes induced by the above-band-gap light (c).

The possibility to observe PA at energies much larger than the exciting photon energy indicates that by irradiation with linearly polarized light not only defects or the scattering centers in the glass can be oriented and reoriented by light but that the main interatomic covalent bonds can be also oriented and reoriented.

The most interesting result which must be explained is the essential difference of reflection spectra for the cases of Xe lamp and Ar^+ laser light excitation (Figs. 6a and 6b). One of the possibilities to understand this difference is demonstrated in Fig. 6c for the simplest case of elemental amorphous selenium. In the initial state, atom 3 is threefold coordinated and atom 10 is onefold coordinated. Following the photoexcitation by the Ar^+ laser light (above-band-gap light) with polarization shown in the figure, lone-pair (LP) electrons oriented parallel to this orientation will predominantly be excited. As a result, atom 10 may form a covalent bond with a neighbouring atom 8, making the latter threefold coordinated. To keep the defect concentration and charge balance, initial threefold coordinated atom 3 decays into a singly coordinated defect and a twofold coordinated "regular" atom. We see here a redistribution of LP and bonding orbitals. Before photoexcitation, the bond between atoms 2 and 3 was covalent (parallel to the x axis), while atoms 8 and 10 had LP orbitals parallel to the z axis. After the photoexcitation, atoms 8 and 10 became bonded by a covalent bond in the z direction, while the bond between atoms 2 and 3 is broken, and two LP orbitals parallel to the x axis are created. As a result, the total number of bonding electrons along the z axis decreases, while the number of non-bonding electrons along the x axis increases, which explains the opposite change in the anisotropy probed at lower and higher energies. In other words, conversion between bonding and non-bonding electrons proceeds.

In the case of broad-spectrum light (Xe lamp), the above-considered process still exists but, additionally, the direct excitation of bonding electrons by the high-energy light quanta becomes possible, resulting in the decrease in the number of bonding electrons in the direction of the light polarization. Since the density of states is larger for bonding electrons than for LP electrons, this latter process will overcompensate a decrease in the number of covalent bonds caused by the excitation with the above-band-gap light, leading to the same change in the sign of anisotropy for both lower and higher energies.

Concluding this part of the paper, we can repeat that, in our opinion, the mechanisms of PA (and of photoinduced gyrotropy) are different for the cases of excitation in different spectral ranges. In case of the above-band-gap excitation, the polarized light orients the natural VAP's existing in the film and creates the photoinduced VAP's that can be quickly oriented. At the sub-band-gap excitation, light creates scattering centers in the glass. Such centers will scatter the light isotropically, anisotropically or gyrotropically depending on the polarization state of the inducing radiation. This process is displayed also in isotropy, anisotropy or gyrotropy of the light transmitted through the sample. At last, in the case of the super-band-gap light, excited radiation is able to orient and reorient the main interatomic covalent bonds of the glass.

3.4. Polarization-dependent photocrystallization

Application of the polarized light resulted in revealing of new peculiarities in the phenomenon of photocrystallization which was studied already during about 30 years [35]. It was shown that the polarization state of excited light influences on the photocrystallization process and on the properties of crystallized samples [13-15,36]. Irradiation of glassy $\text{Se}_{70}\text{Ag}_{15}\text{I}_{15}$, Se and $\text{Se}_{80}\text{Te}_{20}$ films with linearly-polarized He-Ne- and Ar^+ - laser light was shown to result in formation of polycrystalline films with strong optical anisotropy (dichroism), the sign of which is determined by the direction of the electrical vector of light.

Some peculiarities were observed in the processes of reorientation of PA. Reorientation of dichroism in the films studied was characterized by a change of reorientation kinetics and the dichroism sign. At the beginning of the experiment, when the film was amorphous, the vertical polarization vector stimulated increase of positive dichroism while the horizontal polarization vector diminished positive dichroism and led to negative dichroism. In the following stages, the reverse processes were observed as it is demonstrated for the $\text{Se}_{80}\text{Te}_{20}$ films in Fig. 7. Final dichroism was stable, it did not relax in the darkness and could not be erased in the process of annealing at the glass transition temperature.

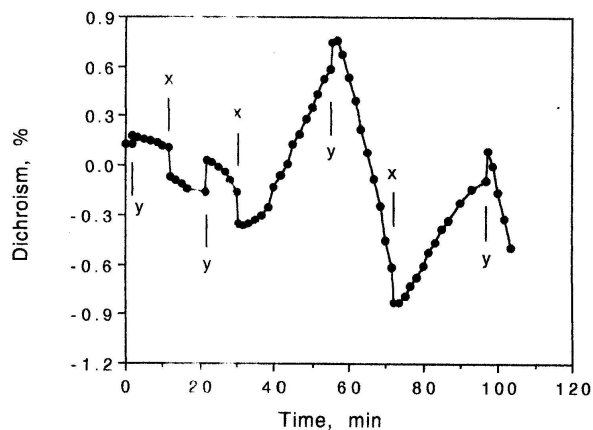


Fig. 7. Kinetics of dichroism generation and reorientation in a thermally treated $\text{Se}_{80}\text{Te}_{20}$ film induced by a linearly polarized He-Ne laser beam with horizontal (x) and vertical (y) directions of electrical vector.

In [37] the phenomenon of laser-induced suppression of the rate of photocrystallization, induced by another laser beam, was observed in glassy Se films. A decisive role of the polarization state of the two laser beams was demonstrated, namely, the suppression effect was observed only when the linear polarization of both beams were parallel to each other. If the polarizations were orthogonal, enhancement of the photocrystallization was observed.

In the $\text{Se}_{80}\text{Te}_{20}$ films, which are characterized by much smaller electrical resistance than the other studied films, we succeeded to observe the photoinduced anisotropy of photoconductivity. The results of study of the $\text{Se}_{80}\text{Te}_{20}$ samples, having special electrodes and working in the bridge-type scheme (which will be shown in Fig. 10 and discussed later) are demonstrated in Fig. 8. It is seen that irradiation of the sample by strong linearly polarized light leads to appearance and growth of photocurrent in the circuit that was preliminary balanced. The change of the exciting light polarization to the orthogonal one was always accompanied by the reversible jumps of the current. Such kinetics of photocurrent is very analogous to the kinetics of the optical dichroism changes that proceed at the polarization-dependent laser crystallization. The early stages can be related towards the kinetics of polarization-dependent laser-induced crystallization and the next stages indicate to the anisotropy of photoconductivity in the photocrystallized $\text{Se}_{80}\text{Te}_{20}$ films.

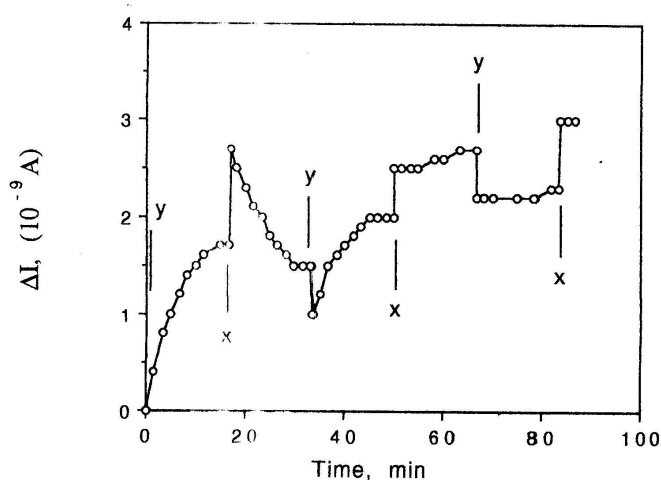


Fig. 8. Kinetics of photocurrent ΔI in a thermally treated $\text{Se}_{80}\text{Te}_{20}$ film induced by a linearly polarized He-Ne laser beam with horizontal (x) and vertical (y) directions of electrical vector.

3.5. Polarization-dependent photodoping

It was shown previously that the Ag-photodoping of As_2S_3 glassy films by linearly polarized light is accompanied by generation of strong dichroism with sign opposite to that generated in Ag-free films [34]. This phenomenon was called by "polarized photodoping". Recently we demonstrated that polarized photodoping by silver is characteristic not only for As_2S_3 films but also for many different chalcogenide glassy films (As_2Se_3 , $\text{As}_{50}\text{Se}_{50}$ and $\text{GeS}_{2.2}$). Some peculiarities were observed in the kinetics of photoinduced dichroism generation. These peculiarities are demonstrated in Fig. 9 for the case of polarized photodoping of $\text{As}_{50}\text{Se}_{50}$ film. When the structure Ag - $\text{As}_{50}\text{Se}_{50}$ is irradiated by linearly polarized He-Ne laser beam of certain polarization, for example, with horizontal direction of the electrical vector, the positive dichroism appeared and increased quickly. Then, after passing through some maximum value, dichroism started to decrease (Fig. 9a). Very unusual was the kinetics of dichroism reorientation. In the first cycles of dichroism reorientation, the horizontal polarization vector stimulated increase of positive dichroism, while the vertical polarization vector decreased the dichroism value, in the following stages the reverse picture was recorded as it is shown in Fig. 9b. This situation reminded us the picture that we observed in case of above-considered photoinduced polarized crystallization and we assumed existence of photocrystallization also in this case. Some experimental confirmations of this assumption were obtained but this fact needs in further investigation. At last we

can say that some interesting results were also obtained at the Zn-photodoping of chalcogenide glassy films.

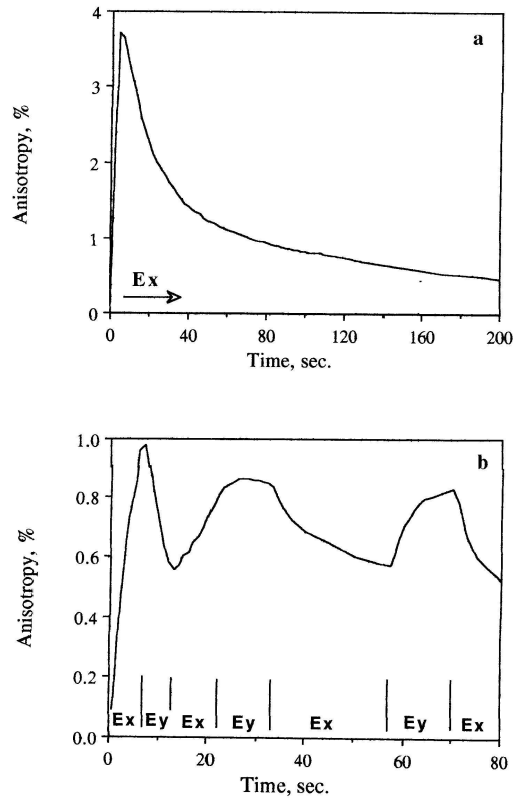


Fig. 9. Kinetics of dichroism generation and reorientation in Ag-photodoped $As_{50}Se_{50}$ film under action of linearly polarized laser light with two orthogonal directions of electrical vector (x and y).

3.6. Photoinduced anisotropy of photoconductivity

In our recent research we demonstrated that the photoinduced optical anisotropy in amorphous $As_{50}Se_{50}$ chalcogenide films is accompanied by the photoinduced anisotropy of photoconductivity and that this effect is optically reversible. 0.3-2.0 μm thick amorphous $As_{50}Se_{50}$ films were prepared by conventional vacuum evaporation technique. A set-up for study of photoconductivity employed one linearly polarized beam of either a He-Ne laser ($P=2.75 W/cm^2$, $\lambda=633 nm$) or an Ar^+ laser ($P=0.3 W/cm^2$, $\lambda=488 nm$) which was used for creating of anisotropy and at the same time for generation of photocarriers. Anisotropy of photoconductivity was measured using films with evaporated golden electrodes, as it is shown in Fig. 10. The space between parallel electrodes 1-2 and 2-3 was 50 μm . The electric circuit was equilibrated by moving the non-polarized beam (shown as a circle 4 in Fig.10) until the nanoammeter G read a zero current. Irradiation with a linearly polarized beam with an electric vector parallel either to 1-2 or to 2-3 electrodes resulted in a differential current detected by a nanoammeter.

Fig. 11 shows the data on anisotropic photoconductivity. Irradiation of sample by the intense linearly polarized beam with an electric vector parallel either to 1-2 or to 2-3 electrodes resulted in a current in the circuit of Fig. 10, which was a differential current between 1-2 and 2-3 electrodes. A change in the polarization state of the inducing light resulted in the respective change of the sign of the resultant current. Kinetics of the change of resultant current was similar to the kinetics of reorientation

of the optical dichroism. Qualitatively similar results were obtained when using the intense linearly polarized Ar^+ laser beam.

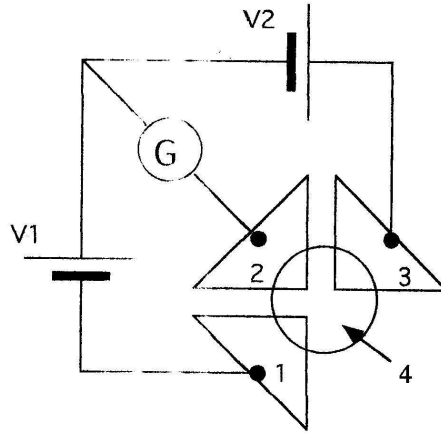


Fig. 10. Layout of electrodes and electrical circuit for measurement of anisotropy of photocurrent. 1,2,3 are the golden electrodes, 4 is a laser beam, G is a nanoampermeter, V1 and V2 are the voltage sources.

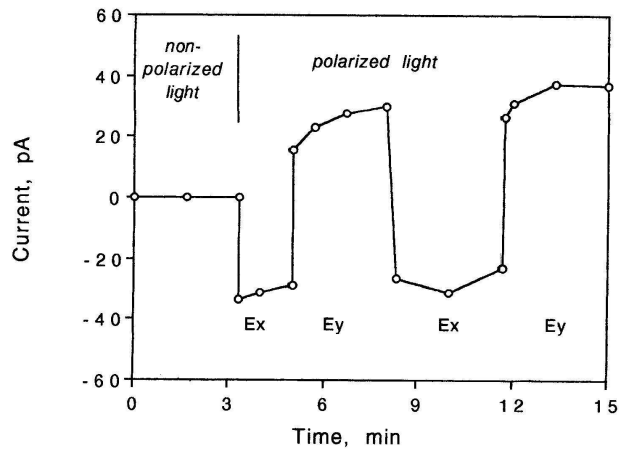


Fig. 11. Kinetics of photocurrent ΔI in $\text{As}_{50}\text{Se}_{50}$ film induced by **Ex** and **Ey** linearly polarized He-Ne laser beam with electrical vector directed parallel or orthogonal to 1-2 electrodes of the sample shown in Fig.10.

One would doubt that the observed change of photocurrent in Fig. 11 is due to photoinduced anisotropy of photoconductivity because the current might appear also due to a subtle shift (drift) of the laser beam relative to electrodes. In order to reject this possibility, we carried out experiment with films CdSe, where photoinduced optical anisotropy was not observed. Large photoconductivity is a property of these films. Irradiation by the non-polarized He-Ne laser beam resulted in gradual increase of the photocurrent up to 400 times. However, irradiation of CdSe film with a linearly polarized He-Ne laser beam with either Ex or Ey polarization did not result in any change of optical absorption or in appearance of anisotropy of photocurrent. This result rules out an effect of laser beam instability (drift) on the data presented in Fig. 11 regarding anisotropy of photoconductivity in $\text{As}_{50}\text{Se}_{50}$ films. To the best of our knowledge, we report a first observation of photoinduced anisotropy of electrical properties and its optical reversibility in chalcogenide films.

3.6. Some other results of interaction of polarized light with chalcogenide glasses

We want to mention shortly two recently discovered and studied effects of polarized light interaction with chalcogenide glassy films. First effect, anisotropic optomechanical effect, consists in appearance of optically controllable, reversible nanocontraction and nanodilatation induced in chalcogenide glassy film ($\text{As}_{50}\text{Se}_{50}$ film) by the linearly polarized light [38]. Very good correlation of this effect with photoinduced dichroism was observed. Mechanism of this effect (also as the mechanism of other photoinduced vectorial effects in chalcogenide glasses) needs in farther study but even now it is clear that it can form the base of a number of mechanical applications driven by polarized light.

Other interesting phenomena were discovered recently in the ion-conducting chalcogenide glasses [39,40]. Studying the Ag-As-S films excited by linearly polarized light, Tanaka, Gotoh and Hayakawa revealed large reversible positive birefringence and anisotropic surface deformations. The anisotropic shape reflected the polarization direction and moreover, the shape changed from a crater-like to anticrater-like form, following change from illumination on the free surface of the film to illumination through a substrate [40]. The authors connected the formation mechanism of such patterns with photoinduced migration of Ag^+ ions in the film.

Concluding this short review paper, we can say that investigation of interaction of polarized light with chalcogenide glasses is in the initial stage. It was demonstrated that irradiation with polarized light can result in many unusual and interesting phenomena in chalcogenide glasses. Examples of such phenomena are polarization-dependent photocrystallization, polarization-dependent metal photodoping, photoinduced anisotropy of photoconductivity, anisotropic optomechanical effect and anisotropic surface deformations which were shortly considered in this paper. Now we are able to give only some speculative explanation to all these phenomena but hope to obtain more detailed understanding in the process of future research. We hope also that some of these phenomena will find interesting application in modern electrooptics and photonics.

Acknowledgments

It is a pleasure to acknowledge the important participation and input of our coauthors V.K.Tikhomirov, A.V.Kolobov, T.Yasuda, K.Tanaka, L.Boehm, M.Mitkova and T.Petkova in this research. This research (No388/00-1) was supported partly by the Israel Science Foundation administrated by the Israel Academy of Science and Humanities.

References

- [1] V. G. Zhdanov, V. K. Malinovskii, *Sov.Tech.Phys.Lett.*, **3**, 387 (1977).
- [2] V. G. Zhdanov, B. T. Kolomiets, V. M. Lyubin, V. K. Malinovskii, *phys.stat.sol.*, **A52**, 621 (1979).
- [3] J. M. Lee, M. A. Paesler, D. E. Sayers, A. Fontaine, *J.Non-Cryst.Sol.*, **123**, 295 (1990).
- [4] V. M. Lyubin, V. K. Tikhomirov, *J.Non-Cryst.Sol.* **135**, 37 (1991).
- [5] V. M. Lyubin, V. K. Tikhomirov, *Avtometrija* No. 4, 14 (1991).
- [6] H. Fritzsche, *Phys.Rev.*, **B52**, 15854 (1995).
- [7] K. Tanaka, M. Notani, H. Hisakuni, *Solid State Commun.*, **95**, 461 (1995).
- [8] S. R. Elliott, V. K. Tikhomirov, *J. Non-Cryst. Sol.*, **198-200**, 669 (1996).
- [9] V. K. Tikhomirov, G. J. Adriaenssens, S. R. Elliott, *Phys. Rev.*, **B55**, R660 (1997).
- [10] V. M. Lyubin, M. L. Klebanov, *Semiconductors*, **32**, 817 (1998).
- [11] P. Hertogen, G. J. Adriaenssens, *J. Non-Cryst.Sol.*, **266-269**, 948 (2000).
- [12] A. V. Kolobov, V. M. Lyubin, V. K. Tikhomirov, *Phil. Mag. Lett.*, **65**, 67 (1992).
- [13] V. Lyubin, M. Klebanov, M. Mitkova, T. Petkova, *Appl. Phys.Lett.*, **71**, 2118 (1997).
- [14] K. Ishida, K. Tanaka, *Phys.Rev.*, **B56**, 206 (1997).
- [15] V. K. Tikhomirov, P. Hertogen, C. Glorieux, G. I. Adriaenssens, *phys.stat.sol.*, **A162**, R1 (1997).
- [16] P. Krecmer, A. M. Moulin, R. J. Stephenson, T. Rayment, M. E. Welland, S. R. Elliott,

- Science **277**, 1799 (1997).
- [17] V. M. Lyubin, V. K. Tikhomirov, J. Non-Cryst. Sol. **114**, 133 (1989).
- [18] S. A. Dembovsky, Sol. St. Commun. **83**, 761 (1992).
- [19] T. Kosa, I. Janossy, Phil. Mag., **B64**, 355 (1991).
- [20] V. K. Tikhomirov, S. R. Elliott, Phys.Rev., **B51**, 5538 (1995).
- [21] E. V. Emelianova, P. Hertogen, V. I. Arkhipov, G. J. Adriaenssens, J. Non-Cryst. Sol., **266-269**, 954 (2000).
- [22] T. Petkova, M. Mitkova, Thin Solid Films, **205**, 25 (1991).
- [23] D. E. Aspnes, J. P. Harbison, A. A. Studna, L. F. Florez, J. Vac. Sci. Technol., **A6**, 1327 (1988).
- [24] V. Lyubin, M. Klebanov, Phys. Rev., **B53**, R 11924 (1996).
- [25] M. Kastner, H. Fritzsche, Philos. Mag., **B37**, 199 (1978).
- [26] E. Vateva, E. Skordeva, D. Arsova, Philos. Mag., **B67**, 225 (1993).
- [27] K. Petkov, B. Dinev, J. Mater. Sci., **29**, 468 (1994).
- [28] M. Klebanov, V. Lyubin, D. Arsova, E. Vateva, V. Pamukchieva, Physica B (2001), in press.
- [29] V. M. Lyubin, V. K. Tikhomirov, J. Non-Cryst. Sol., **137-138**, 993 (1991).
- [30] V. K. Tikhomirov, Fizika i Tekhnika Poluprovodnikov, **26**, 1415 (1992).
- [31] V. Lyubin, M. Klebanov, S. Rosenwaks, V. Volterra, J. Non-Cryst. Sol., **164-166**, 1165 (1993).
- [32] M. Klebanov, V. Lyubin. Physica, **B245**, 206 (1998).
- [33] A. V. Kolobov, V. Lyubin, T. Yasuda, M. Klebanov, K. Tanaka, Phys. Rev., **B55**, 8788 (1997).
- [34] A. V. Kolobov, V. M. Lyubin, V. K. Tikhomirov, Phil. Mag. Lett. **65**, 67 (1992).
- [35] J. Dresner, G. B. Stringfellow, J. Phys. Chem. Sol., **29**, 303 (1968).
- [36] V. Lyubin, M. Klebanov, M. Mitkova, Appl. Surf. Sc., **154-155**, 135 (2000).
- [37] A. Roy, A. V. Kolobov, K. Tanaka, J. Appl. Phys., **83**, 4951 (1998).
- [38] P. Krecmer, A. M. Moulin, R. J. Stephenson, T. Rayment, M. E. Welland, S. R. Elliott, Science, **277**, 1799 (1997).
- [39] K. Tanaka, T. Gotoh, H. Hayakawa, Appl. Phys. Lett., **75**, 226 (1999).
- [40] T. Gotoh, K. Tanaka, J. Appl. Phys, **89**, 4703 (2001).